

1 Sunlight Promotes Fast Release of Hazardous Cadmium
2 from Widely-Used Commercial Cadmium Pigment

3 Huiting Liu¹, Han Gao¹, Mingce Long², Heyun Fu¹, Pedro J.J. Alvarez³, Qilin Li³, Shourong Zheng¹,
4 Xiaolei Qu^{1*}, Dongqiang Zhu⁴

5 ¹State Key Laboratory of Pollution Control and Resource Reuse, School of the Environment, Nanjing
6 University, Jiangsu 210023, China

7 ²School of Environment Science and Engineering, Shanghai Jiao Tong University, Shanghai 200240,
8 China

9 ³Department of Civil and Environmental Engineering, Rice University, Houston TX 77005, United
10 States

11 ⁴School of Urban and Environmental Sciences, Peking University, Beijing 100871, China

12 * Corresponding author Xiaolei Qu, phone: +86-025-8968-0256; email: xiaoleiqu@nju.edu.cn

13

14

15 **Abstract**

16 Cadmium pigments are widely used in the polymer and ceramic industry. Their potential
17 environmental risk is under debate, being the major barrier for appropriate regulation. We show that
18 83.0 ± 0.2 % of hazardous cadmium ion (Cd^{2+}) was released from the commercial cadmium
19 sulfoselenide pigment (i.e., cadmium red) in aqueous suspension within 24 h under simulated sunlit
20 conditions. This photo-dissolution process also generated sub-20 nm pigment nanoparticles. Cd^{2+} release
21 is attributed to the reactions between photogenerated holes and the pigment lattices. The photo-
22 dissolution process can be activated by both ultraviolet and visible light in the solar spectrum.
23 Irradiation under alkaline conditions or in the presence of phosphate and carbonate species resulted in
24 reduced charge carrier energy or the formation of insoluble and photo-stable cadmium precipitates on
25 pigment surfaces, mitigating photo-dissolution. Tannic acid inhibited the photo-dissolution process by
26 light screening and scavenging photogenerated holes. The fast release of Cd^{2+} from the pigment was
27 further confirmed in river water under natural sunlight, with 38.6 ± 0.1 % of the cadmium released
28 within 4 h. Overall, this study underscores the importance to account for photochemical effects to
29 inform risk assessments and regulations of cadmium pigments which are currently based on their low
30 solubility.

31

32 **Introduction**

33 Cadmium pigments, including cadmium sulfide, cadmium selenide, and cadmium sulfoselenide, are
34 widely used in the polymer and ceramic industries owing to their heat stability, chemical resistance,
35 dispersibility, opacity, tinting strength, and brilliance.^{1, 2} They are especially preferred in processes or
36 applications involving elevated temperatures in which organic pigments are unstable. The annual global
37 consumption of cadmium pigments exceeds 2,500 tons, with 90 % used in plastics and 9 % in ceramics.²
38 There is a long debate on whether cadmium pigments pose a genuine risk to human health and the

39 environment.^{1,2} Cadmium ion (Cd^{2+}) is known to cause acute toxicity based on short-term animal tests,
40 and is a probable human carcinogen.³ Thus the dissolution of cadmium pigments and consequent release
41 of hazardous Cd^{2+} are key processes that control their potential environmental impacts. Previous risk
42 assessments suggested that the use of cadmium pigments poses little risk to humans and the
43 environment (except in occupational settings) due to their extremely low solubility ($K_{\text{sp,CdS}} = 7.94 \times 10^{-27}$
44 and $K_{\text{sp,CdSe}} = 6.31 \times 10^{-36}$),⁴ and consequently low bioavailability.⁵⁻⁸ Because of insufficient fate,
45 transport, and toxicological studies, current cadmium pigment regulations are based on the
46 precautionary principle.¹ For example, the European Union (EU) prohibits the use of cadmium pigments
47 in 16 plastics with exemptions (see Regulation No. 494/2011). In China and EU, cadmium pigments are
48 recommended to pass extraction tests for Cd^{2+} , < 0.1 wt % (Standards ISO 4620:1986, BS 6857-1987,
49 and HG 2351-1992). However, these presumably conservative regulations may still underestimate
50 associated risks by overlooking photochemical processes that enhance Cd^{2+} release.

51 The band gap of CdS and CdSe are 2.5 eV and 1.8 eV, respectively.⁹ Cadmium sulfoselenide is the
52 solid solution of CdS and CdSe, whose color can be fine-tuned from orange to red by increasing the
53 amount of selenium.^{2,10} Its band gap decreases from 2.5 eV to 1.8 eV with increasing Se content.^{9,11}
54 Thus cadmium pigments are photoactive under sunlight and are proposed to be used in photovoltaic
55 devices to harvest solar energy.^{12,13} However, for many metal-containing semiconductor photocatalysts,
56 photo-corrosion process will lead to the dissolution and consequent release of metals.¹⁴⁻¹⁹

57 Photo-corrosion of CdS and CdSe nanoparticles/quantum dots and subsequent release of Cd^{2+} were
58 investigated in previous studies.^{14,15,20-27} The process can be induced by oxidative phototransients
59 including photogenerated holes and reactive oxygen species (ROS). However, these studies were carried
60 out using cadmium chalcogenide nanoparticles mostly in simple solution chemistry, and cannot be
61 extrapolated to infer on the behavior of commercial cadmium pigments in natural settings. The photo-
62 degradation of CdS pigment in air has also been studied by analyzing historical oil paintings in aim to
63 minimize their deterioration process.²⁸⁻³⁰ The discoloration of CdS pigment was attributed to photo-

64 induced oxidation over centuries, which yielded $\text{CdSO}_4 \cdot x\text{H}_2\text{O}$ and other cadmium species (e.g., CdCO_3)
65 by secondary reactions. Nevertheless, our understanding of the photo-dissolution process of modern
66 commercial cadmium pigments in natural aquatic systems is still limited, which hinders risk assessment
67 and science-based regulation of these pigments and related colored consumer products.

68 Herein, we examine the photo-dissolution of a commercial cadmium sulfoselenide pigment (i.e.,
69 cadmium red) under simulated sunlight at neutral pH, mimicking natural conditions. The band gap of
70 the pigment and the phototransients generated during irradiation were determined to understand its
71 photochemistry within the solar spectrum. The influence of solution chemistry including pH, phosphate,
72 carbonate, and tannic acid on the photo-dissolution kinetics was further examined to inform the
73 environmental release process. The photo-dissolution of cadmium pigments was also examined in river
74 water under natural sunlit conditions to corroborate our findings. In addition to discerning the photo-
75 induced dissolution mechanism, we underscore the importance to consider photochemical processes to
76 accurately assess the associated risks and inform the regulatory process.

77

78 **Materials and Methods**

79 Commercial cadmium sulfoselenide pigment powder (cadmium red) was purchased from Kela Co.,
80 Ltd., China. Dimethyl sulfoxide (DMSO, $\geq 99.0\%$), sodium chloride (NaCl , $\geq 99.5\%$), sodium
81 carbonate (Na_2CO_3 , $\geq 99.8\%$), sodium thiosulfate pentahydrate ($\text{Na}_2\text{S}_2\text{O}_3 \cdot 5\text{H}_2\text{O}$, $\geq 99\%$) and sodium
82 sulfate (Na_2SO_4 , $\geq 99\%$) were purchased from Nanjing Chemical Reagent Co., Ltd., China. 5,5-
83 Dimethyl-1-pyrroline-N-oxide (DMPO, $\geq 97\%$) was obtained from J&K Scientific Ltd., USA. Sodium
84 selenite (Na_2SeO_4 , $\geq 98\%$) was purchased from Chengdu Micxy Chemical Co., Ltd., China. Methyl
85 viologen dichloride hydrate (MV^{2+} , $\geq 98\%$), sodium phosphate (Na_3PO_4 , 96%), sodium selenite
86 pentahydrate ($\text{Na}_2\text{SeO}_3 \cdot 5\text{H}_2\text{O}$, $\geq 90\%$), 2,3-bis(2-methoxy-4-nitro-5-sulfophenyl)-2*H*-tetrazolium-5-
87 carboxanilide (XTT, $> 90\%$), terephthalic acid (TPA, 98%), *N,N*-diethyl-*p*-phenylenediamine sulfate
88 salt (DPD, $\geq 99\%$), and horseradish peroxidase (HRP, ≥ 250 units/mg) were purchased from Sigma-

89 Aldrich, USA. Tannic acid (95 %) was purchased from Acros Organics, USA. All solutions were
90 prepared using deionized water (18.2 MΩ•cm at 25 °C) obtained from an ELGA Labwater system
91 (PURELAB Ultra, ELGA LabWater Global Operations, UK).

92 **Irradiation experiments.** The stock suspension of commercial cadmium sulfoselenide pigment was
93 prepared by mixing 10 mg pigment with 100 mL deionized water and sonicated using a flat-tip probe
94 sonicator (JY92-IIN, Ningbo Scientz Biotechnology Co., Ltd., China) for 10 min. The sonication probe
95 was operated at a power of 65 W with a mode of five-second sonication and five-second pause.

96 The sunlight irradiation was simulated by a 50 W Xe lamp (CEL-HXF300, AULTT, China) shining
97 from the top of a cylindrical cell which was equipped with a water-circulating jacket at 20 ± 0.1 °C
98 (DC0506, Shanghai FangRui Instrument Co., Ltd., China). The irradiation energy at the water surface
99 was 202 mW/cm² as measured by a radiometer (CEL-NP2000-2, AULTT). The detailed information
100 regarding the irradiation system can be found in Figure S1. The lamp spectrum was similar to that of
101 natural sunlight with the wavelength > 300 nm as measured by a spectrometer (USB2000+, Ocean
102 Optics, FL, USA) (Figure S2). In the irradiation experiments, twenty milliliter cadmium sulfoselenide
103 pigment stock suspension (100 mg/L) and 10 mL NaCl stock solution (20 mM) were mixed and diluted
104 to 200 mL with deionized water in a 250 mL beaker, yielding a suspension containing 10 mg/L
105 cadmium sulfoselenide pigment and 1 mM NaCl. The beaker was then placed in the cylindrical cell for
106 temperature control. The suspension was stirred at 100 rpm during the irradiation experiments. NaCl
107 added in the suspension was used to simulate the ionic strength in freshwater systems. The un-adjusted
108 pH of the mixture was 6.77 ± 0.33 . During the irradiation, 4 mL suspension was withdrawn periodically
109 from the beaker and filtered using ultrafiltration membranes (Amicon Ultra-15 3 kD, Millipore, MA,
110 USA) to separate the dissolved ions from the particles. The Cd²⁺ concentration was determined by
111 atomic absorption spectrophotometry (AAS, M6, Thermo, USA). The concentrations of other ions
112 presented in irradiated pigment suspensions were determined by ion chromatography (ICS-1000,
113 Dionex, USA) with a Dionex IonPac AS11-HC analytical column (250 mm × 4 mm). Dark controls

139 glass plate (Huanan Xiangcheng Co. Ltd., China, 2.5 cm × 2.5 cm, 1.1 mm thick, sheet resistance of 6-8
140 Ω/in^2). The electrode was then dried at 60 °C for 2 h. The electrolyte was 0.5 M Na₂SO₄ aqueous
141 solution with pH of 5.5. The ac amplitude and frequency were set to be 5 mV and 1.5 KHz, respectively.
142 The ζ -potential of the pigment particles was measured by phase analysis light scattering (PALS) using a
143 ZEN 3500 Zetasizer Nano ZS (Malvern, Worcestershire, UK). Each sample was measured five times at
144 25 °C in a folded capillary cell (Malvern, Worcestershire, UK).

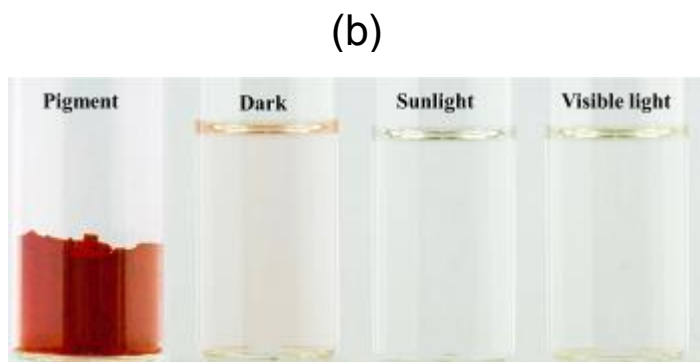
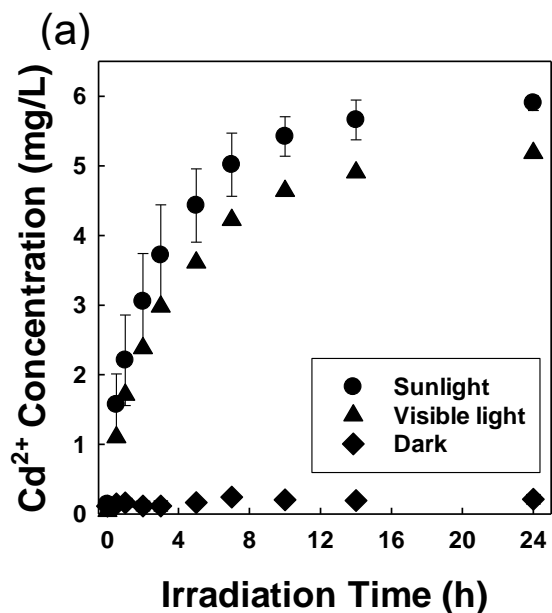
145 **ROS determination.** The production of superoxide ($\text{O}_2^{\cdot-}$), hydroxyl radical ($\cdot\text{OH}$), and hydrogen
146 peroxide (H_2O_2) by pigment suspensions was measured using probe molecules as described
147 previously.³¹⁻³⁵ Superoxide generation was quantified by the formation of XTT formazan from XTT at
148 an initial concentration of 0.05 mM. XTT formazan was quantified by its absorption at 475 nm using a
149 UV-vis spectra. The extinction coefficient of XTT formazan is 21600 $\text{M}^{-1}\text{cm}^{-1}$.^{31, 34} Hydroxyl radical
150 production was quantified by monitoring the degradation of *p*CBA.³²⁻³⁴ The *p*CBA concentration was
151 measured at a detection wavelength of 254 nm using a high performance liquid chromatography (HPLC,
152 Agilent 1100, Agilent Technologies, USA) with a Zorbax Eclipse XDB-C18 column (Agilent). The
153 mobile phase was 30 % acetonitrile and 70 % 0.1 wt% phosphoric acid at a flow rate of 1 mL/min. H_2O_2
154 generation was measured by the HRP (5 mg/L) catalyzed oxidation of DPD (1mM).³⁵ The stable
155 oxidation product, DPD^{*+} , was measured by the UV-vis absorbance at 551 nm. The spin-trapping
156 electron spin resonance (ESR) spectra were recorded on a Bruker EMX-10/12 spectrometer (Germany)
157 at room temperature with X-band, microwave power of 20 mW, sweep width of 200 G, modulation
158 width of 1 G, modulation frequency of 100 kHz.

159 **Results and Discussion**

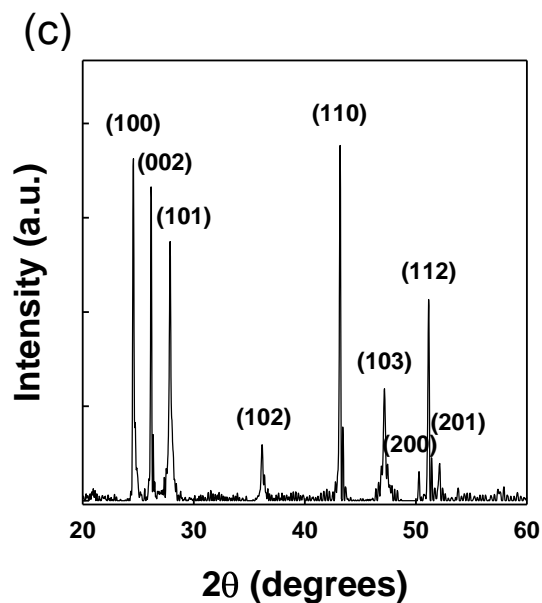
160 **Simulated sunlight exposure results in rapid release of Cd²⁺ from commercial cadmium** 161 **sulfoselenide pigment**

162 The dissolution kinetics of a representative cadmium pigment, cadmium sulfoselenide ($\text{CdS}_x\text{Se}_{1-x}$)
163 was examined to assess its ability to release hazardous Cd²⁺. The commercial cadmium sulfoselenide

164 pigment used here was a fine powder with brilliant red color (Figure 1). The SEM and TEM
165 micrographs showed that pigment particles were quasi-spherical with a number average diameter of
166 186.1 ± 95.8 nm based on TEM micrographs (Figure 2). The commercial pigment can be readily
167 dispersed in water (Figure 1b). The observed colloidal stability can be attributed to the small size and
168 negative surface charge of the pigment particles with a ζ -potential of -24.37 ± 1.48 mV (electrophoretic
169 mobility of -1.91 ± 0.12 $\mu\text{m}\cdot\text{cm}/\text{Vs}$), which facilitates their colloidal stability through electrostatic
170 repulsion as suggested by the Derjaguin-Landau-Verwey-Overbeek theory.^{36, 37} The XRD pattern of the
171 commercial pigment is shown in Figure 1c. The XRD spectrum has sharp peaks corresponding to the
172 crystal structure of cadmium sulfoselenide, including 2θ at 24.66° (100), 26.28° (002), 27.99° (101),
173 36.34° (102), 43.30° (110), 47.28° (103), 50.38° (200), 51.28° (112), and 52.19° (201).^{12, 38} ICP-MS
174 measurements suggested the atomic ratio of S:Se of the pigment was 1.9 ± 0.1 .

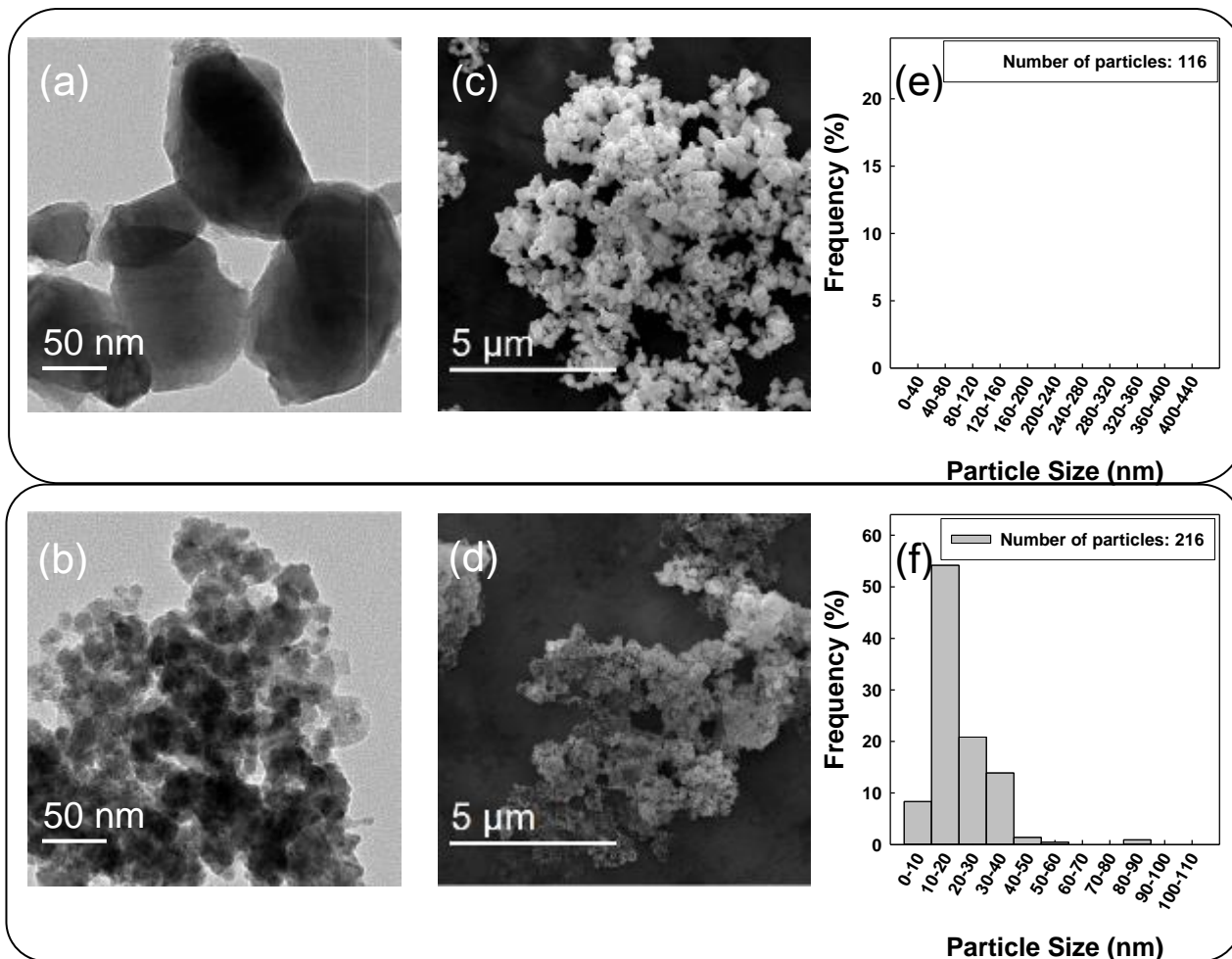


175



176

177 Figure 1. (a) Cadmium release kinetics of 10 mg/L commercial cadmium sulfoselenide pigment in 1
178 mM NaCl solution at initial pH of 6.77 ± 0.33 under dark, simulated sunlight (202 mW/cm^2), and
179 visible light irradiation (152 mW/cm^2). Error bars represent \pm one standard deviation from the average
180 of triplicate tests; (b) photos of the commercial cadmium sulfoselenide pigment sample used in this
181 work and its suspension (10 mg/L) in 1 mM NaCl solution after 24 h under dark, simulated sunlight,
182 and visible light conditions; (c) XRD spectrum of commercial cadmium sulfoselenide pigment.



183

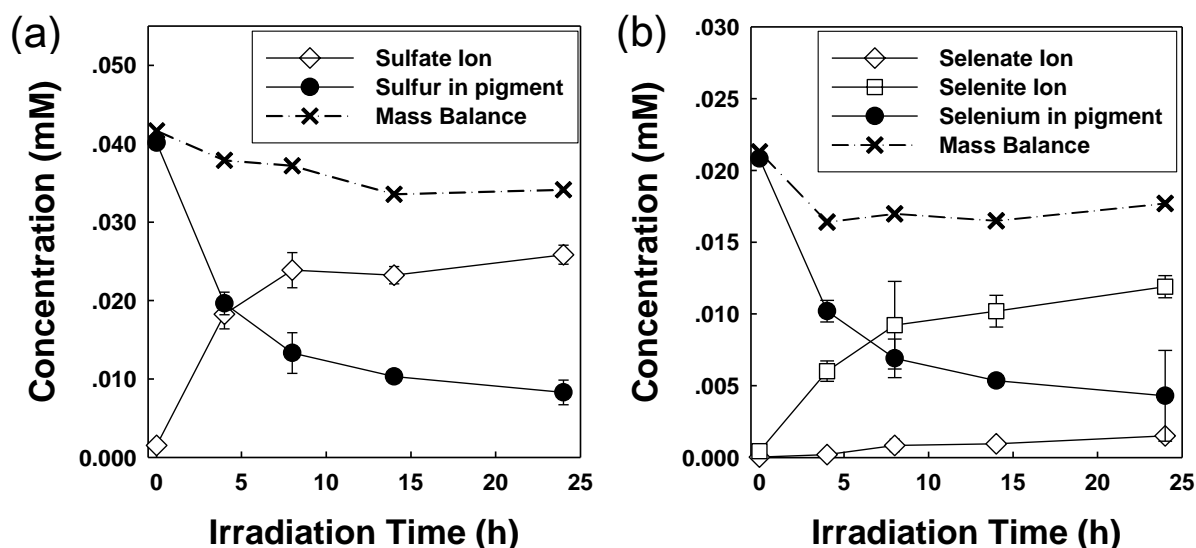
184 Figure 2. Morphology and size distribution of commercial cadmium sulfoselenide pigment particles
 185 before and after 7-h simulated sunlight exposure. TEM micrographs of commercial cadmium
 186 sulfoselenide pigment particles (a) before and (b) after sunlight exposure; SEM micrographs of
 187 commercial cadmium sulfoselenide pigment particles (c) before and (d) after sunlight exposure; size
 188 distribution of commercial cadmium sulfoselenide pigment particles (e) before and (f) after sunlight
 189 exposure based on TEM micrographs.

190

191 The release kinetics of Cd^{2+} from cadmium sulfoselenide pigment was determined under both dark
 192 and simulated sunlight irradiation (Figure 1a, see the release kinetics for other cadmium sulfoselenide
 193 pigments from different vendors in Figure S3). A small amount of Cd^{2+} , 0.21 ± 0.07 mg/L (< 3.0 % of
 194 the total Cd), was released in the dark condition within 24 h. It can be attributed to the dissolution of

195 cadmium sulfoselenide or the Cd^{2+} release during the dispersion process by sonication. Considering the
196 extremely low solubility of CdS (solubility product constant, $K_{\text{sp}} = 7.94 \times 10^{-27}$) and CdSe ($K_{\text{sp}} =$
197 6.31×10^{-36}),⁴ the majority of Cd^{2+} released in dark condition is expected to be the latter. However, fast
198 and significant release of Cd^{2+} was observed in the presence of simulated sunlight. The concentration of
199 Cd^{2+} in the suspension increased to 5.01 ± 0.45 mg/L within a 7-h irradiation, and to 5.90 ± 0.10 mg/L
200 at the end of the 24-h irradiation test. This means that 83.0 ± 0.2 % of the total cadmium was released,
201 far exceeding the 0.1 % limit stipulated by ISO Standard 4620:1986. The pseudo-second-order reaction
202 rate constant was 3.0 L/(mmol·h) ($R^2 = 0.93$), 334 times higher than that under dark conditions. The rate
203 constant decreased from 3.0 to 1.5 L/(mmol·h) ($R^2 = 0.95$) after a cut-off filter was applied to remove
204 the UV component of the simulated sunlight (Figure 1a). This indicates that the photo-dissolution can be
205 induced by visible light in the solar spectrum which comprises the majority of the photon flux in solar
206 irradiation.³⁹

207 During irradiation, the color of the cadmium sulfoselenide pigment suspension changed from red to
208 transparent, supporting the fast photo-dissolution of the pigment (Figure 1b). The ζ -potential of the
209 pigment particles was stable at -26.15 ± 1.24 mV (Figure S4). TEM and SEM micrographs of pigment
210 particles suggest that particle size was significantly decreased owing to the photo-dissolution process
211 (Figure 2a-d). Based on the size distribution diagrams (Figure 2e and 2f), the number average size of the
212 pigment particles sharply decreased from 186.1 ± 95.8 nm to 19.7 ± 8.7 nm after 7-h irradiation. The
213 size distribution also became narrower (i.e., less heterogeneous) after irradiation. The majority of the 7-
214 h-irradiated pigment particles had sizes within the range of 10 ~ 20 nm.



215

216 Figure 3. (a) The concentrations and mass balance of sulfur species, including sulfur in the pigment and

217 sulfate ion (SO_4^{2-}), as a function of simulated sunlight irradiation time at initial pH of 6.77 ± 0.33 . (b)

218 The concentrations and mass balance of selenium species, including selenium in the pigment, selenite

219 ion (SeO_3^{2-}), and selenate ion (SeO_4^{2-}), as a function of simulated sunlight irradiation time.

220

221 The release of sulfur and selenium species and their mass balance were examined during the photo-

222 dissolution of commercial cadmium sulfoselenide pigment (Figure 3). The solution concentration of

223 SO_4^{2-} increased with decreasing sulfur remaining in the pigment (Figure 3a). No SO_3^{2-} or S was detected

224 using ion chromatography and HPLC, respectively. The mass balance of sulfur species was 81.8 % at 24

225 h. Similar analysis was applied to selenium species (Figure 3b). Both SeO_3^{2-} and SeO_4^{2-} were detected

226 as reaction products, with SeO_4^{2-} being the major product and SeO_3^{2-} being the intermediate product.

227 The mass balance of selenium species was 83.1 % at 24 h.

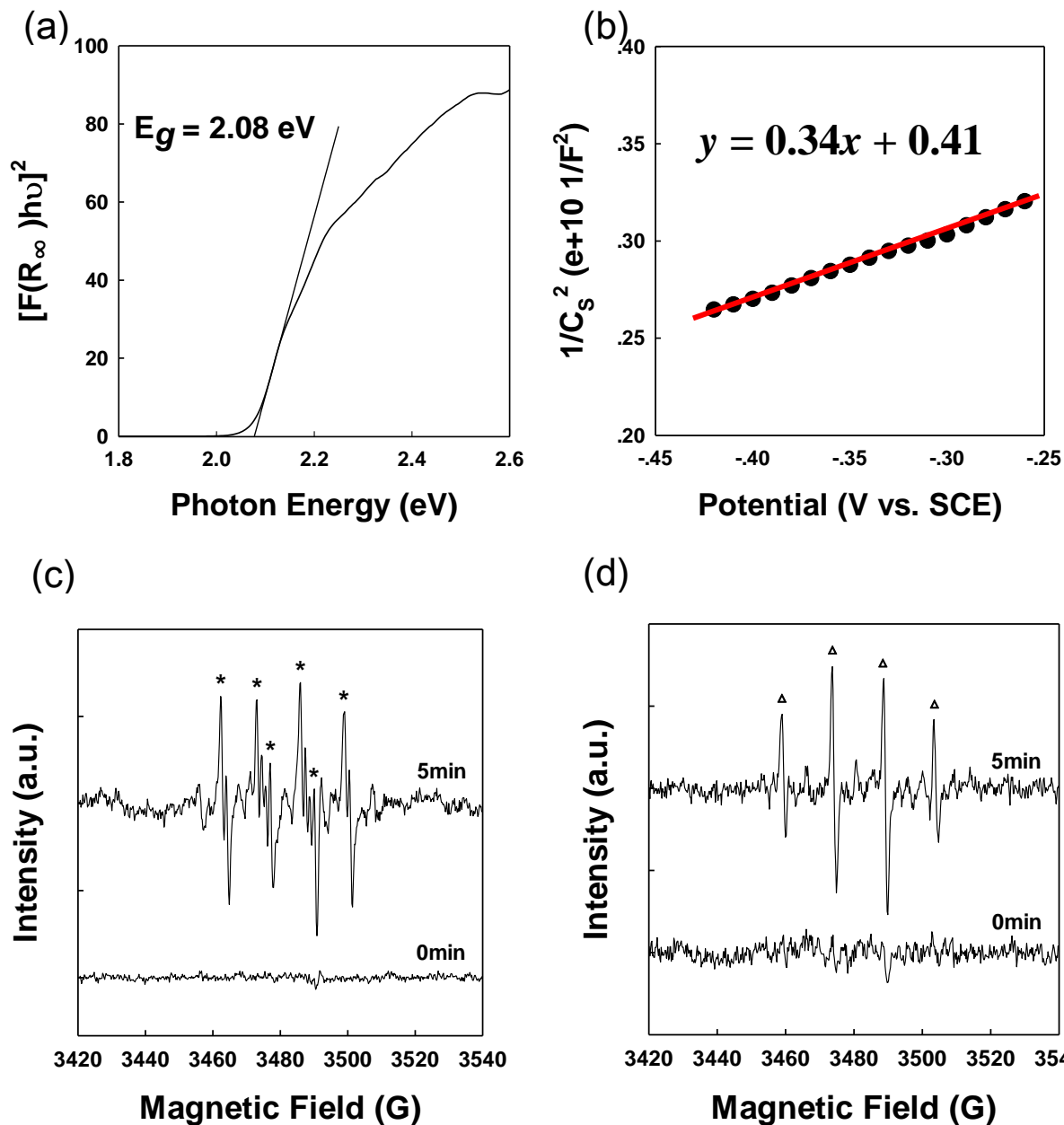
228 Mechanisms of the photo-dissolution of commercial cadmium sulfoselenide pigments

229

230

231

232

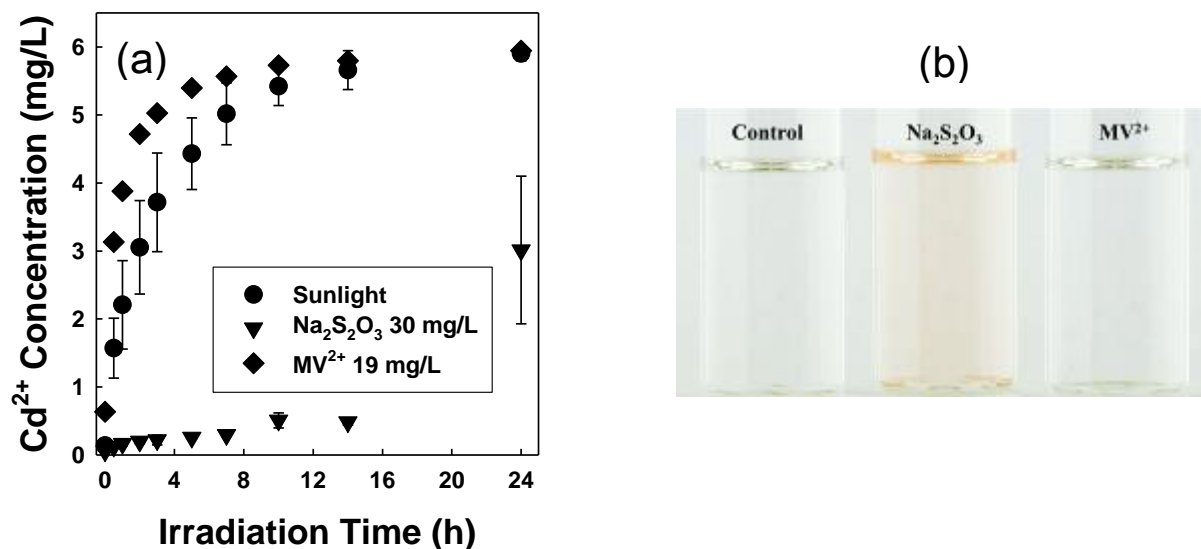


233

234

235 Figure 4. (a) Kubelka-Munk function, $(F(R_\infty)/\text{hu})^2$, as a function of photon energy. (b) Mott-Schottky
 236 plot of the commercial cadmium sulfoselenide pigment. (c) ESR spectra recorded under simulated
 237 sunlight irradiation with 10 mg/L commercial cadmium sulfoselenide pigment and 100 mM spin trap
 238 DMPO in 80% DMSO, indicating the generation of superoxide ($\text{O}_2^{\cdot-}$). (d) ESR spectra recorded during
 239 simulated sunlight irradiation with 10 mg/L commercial cadmium sulfoselenide pigment and 100 mM
 240 spin trap DMPO in water, indicating the generation of hydroxyl radicals ($\cdot\text{OH}$).

241



242

243 Figure 5. (a) Cadmium release kinetics of 10 mg/L commercial cadmium sulfoselenide pigment in 1
 244 mM NaCl solution at initial pH of 6.86 ± 0.43 in the presence of 30 mg/L Na₂S₂O₃ or 19 mg/L methyl
 245 viologen (MV²⁺) under simulated sunlight (202 mW/cm²). Error bars represent \pm one standard deviation
 246 from the average of triplicate tests. (b) Photos of 10 mg/L commercial cadmium sulfoselenide pigment
 247 in 1 mM NaCl solution in the presence of 30 mg/L Na₂S₂O₃ or 19 mg/L MV²⁺ after 24 h simulated
 248 sunlight irradiation.

249

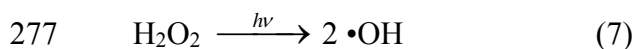
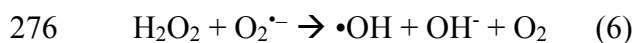
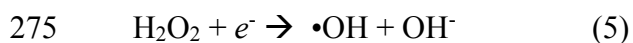
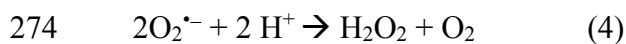
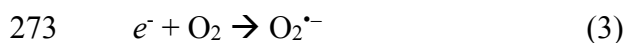
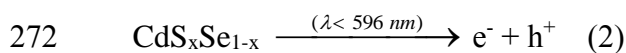
250 To better understand the photochemistry of commercial cadmium sulfoselenide pigment in the solar
 251 spectrum, its band gap energy (E_g) was determined by DRS (Figure 4a). The commercial pigment
 252 showed strong light absorbance up to ~ 600 nm. Its DRS spectrum was transformed to the Kubelka-
 253 Munk function, $(F(R_\infty)h\nu)^2$, versus the photon energy plot as shown in Figure 4a.^{40, 41}

254
$$F(R_\infty) = (1-R)^2 / (2R) \quad (1)$$

255 In which, R is the reflectance, h is Planck's constant, and ν is the light frequency. The E_g was
 256 determined to be 2.08 eV by extrapolating the steepest slope to the x axis (Figure 4b).⁴¹ This value is
 257 generally consistent with the typical range of the E_g of cadmium sulfoselenide nanocrystals.⁹ Thus,
 258 commercial cadmium sulfoselenide pigment used in this study can be activated by irradiation

259 wavelength < 596 nm (i.e., 2.08 eV), which covers the major part of the solar spectrum. This agrees
260 well with the fact that the photo-dissolution kinetics was still fast after filtering the UV light in the
261 simulated sunlight (Figure 1a).

262 The flat-band potential of the pigment was determined using the Mott-Schottky method (Figure 4b).
263 The slope of the linear regression is positive, indicating that the cadmium sulfoselenide pigment is a n-
264 type semiconductor, for which the flat-band potential is close to the conduction band potential.⁴² The
265 conduction band potential of the cadmium pigment used in this study is -0.97 V vs. NHE (i.e., -1.21 V
266 vs. SCE) at pH 5.5 as determined by the linear extrapolation method. The position of conduction band
267 edge is a function of the solution pH, ~ 0.059 V/pH.⁴³ Thus, the conduction band potential is estimated
268 to be -1.06 V at pH 7.0. The valence band is calculated to be 1.02 V based on the conduction band
269 potential and E_g. When excited by incident photons with energy higher than the band gap energy,
270 cadmium sulfoselenide pigment generates electron-hole pairs which migrate to the surface of particles
271 (Equation 2).



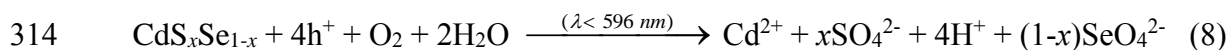
278 Colloidal semiconductors usually contain a large number of surface defect sites, which can trap
279 charge carriers upon excitation.⁴⁴ Some of these charge carriers will react with surrounding molecules to
280 form phototransients. The conduction band potential of the pigment is more negative than the redox
281 potential of O₂/ O₂^{•-} (-0.28 V vs. NHE), thus the photogenerated electrons can transfer to O₂ and form
282 O₂^{•-}. We carried out ESR experiments under simulated sunlight irradiation using DMPO as a spin trap
283 to detect these phototransients. In the presence of 10 mg/L pigment and 80 % DMSO as the •OH

284 quencher, a characteristic fingerprint of the DMPO•OO(H) adduct ($a_N = 12.7$ G, $a_H = 10.3$ G) was
285 observed, indicating the generation of $O_2^{\bullet-}$ (Figure 4c).⁴⁵ Control test suggested that there was no ESR
286 peaks in the same sample without simulated sunlight irradiation. Thus the electrons generated by the
287 pigment can combine with oxygen molecules to yield $O_2^{\bullet-}$ (Equation 3). The production of $O_2^{\bullet-}$ was also
288 examined by molecular probe, XTT, which can readily react with $O_2^{\bullet-}$, producing XTT formazan.³¹ The
289 formation of XTT formazan in the pigment suspension was a function of irradiation time (Figure S5a).
290 It is worth noting that the XTT assay might not be specific to $O_2^{\bullet-}$ in some cases under UV irradiation.⁴⁶
291 Nevertheless, the generation of XTT formazan was almost completely inhibited in the presence of
292 superoxide dismutase (Figure S5b), confirming the generation of $O_2^{\bullet-}$.⁴⁶

293 In 10 mg/L pigment water suspension, we observed an ESR pattern consisting of a 1:2:2:1 quartet
294 with $a_N = a_H = 14.9$ G under simulated sunlight, which is the hallmark for the DMPO•OH adduct (Figure
295 4d), indicating the generation of •OH.⁴⁵ By using molecular probe, *p*CBA, the generation of •OH was
296 confirmed in the illuminated pigment suspension (Figure S5c).^{32, 33} The valence band potential of the
297 pigment (+1.02 V vs. NHE) is lower than the redox potential of •OH/H₂O (+2.27 V vs. NHE) and
298 •OH/OH⁻ (+1.99 V vs. NHE). Thus, the generation of •OH was not caused by the reactions between
299 holes and H₂O or surface-bound OH⁻. H₂O₂ was detected in the irradiated pigment suspension as shown
300 in Figure S5d, which was the product of the disproportionation of $O_2^{\bullet-}$ (Equation 4). Therefore, the
301 detected •OH was most likely formed through the H₂O₂ reduction pathway (Equation 5-6).⁴⁷

302 The valence band edge (+1.02 V vs. NHE) is higher than the standard potential for anodic dissolution
303 of cadmium chalcogenide, around +0.32 V vs. NHE,⁴⁸ leading to the corrosion of pigment surface sites
304 by photogenerated holes.^{15, 19, 49, 50} To test this hypothesis, we added electron/hole scavengers into the
305 reaction system. The photo-dissolution of the pigment was completely inhibited initially by the addition
306 of 30 mg/L Na₂S₂O₃, a hole scavenger,⁵¹ highlighting the predominant role of photogenerated holes
307 (Figure 5). The release of Cd²⁺ was observed after 7-h irradiation likely due to the consumption of
308 Na₂S₂O₃. On the other hand, the photo-dissolution of Cd²⁺ was enhanced in the presence of an electron

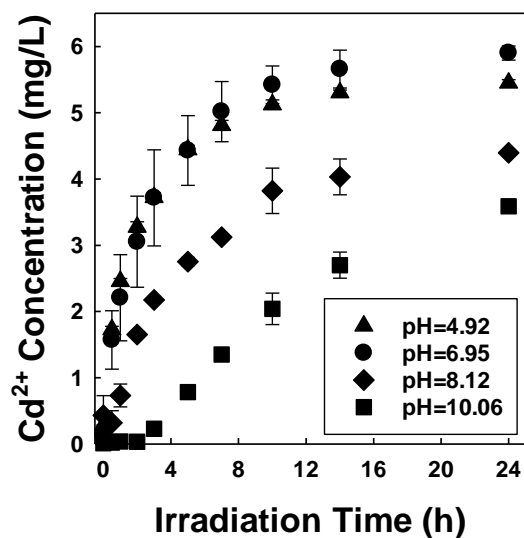
309 scavenger, MV^{2+15} (Figure 5). The MV^{2+} quickly reacted with photogenerated electrons, decreasing the
310 recombination of photogenerated electron-hole pairs and consequently leaving more holes involved in
311 the reactions with pigment lattices.^{15, 22} Based on the evidence presented above as well as earlier reports
312 on the photo-corrosion of CdS and CdSe nanocrystals, we proposed a mechanism for the sunlight-
313 induced dissolution of commercial cadmium sulfoselenide pigments:



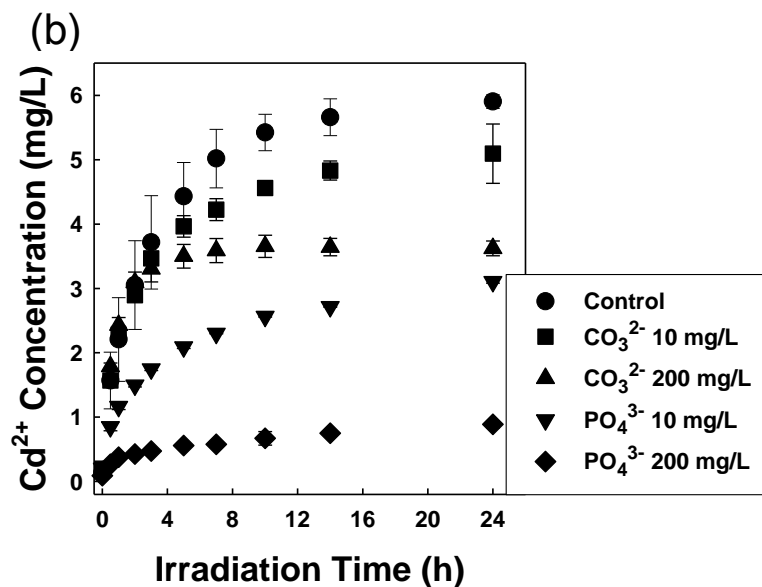
315 **Impact of water chemistry on the photo-dissolution kinetics of commercial cadmium**
316 **sulfoselenide pigments**

317

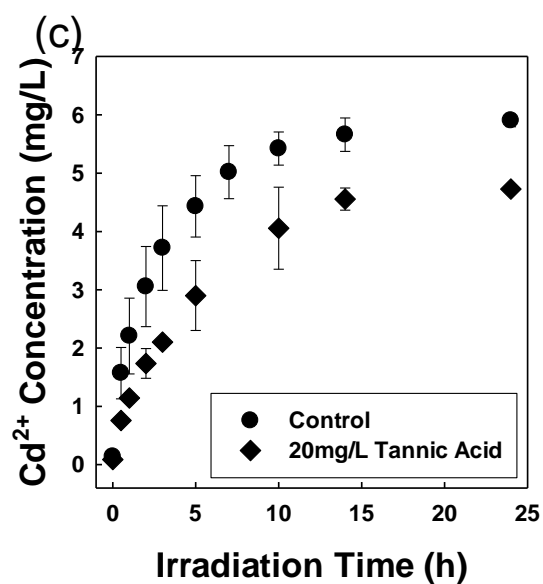
(a)



318



319



320

321 Figure 6. Dissolution kinetics of 10 mg/L commercial cadmium sulfoselenide pigment in 1 mM NaCl
 322 solution under simulated sunlight irradiation (a) at various initial pH, (b) in the presence of PO₄³⁻ or
 323 CO₃²⁻ species at initial pH of 6.90 ± 0.30, and (c) in the presence of tannic acid at initial pH of 6.51 ±
 324 0.10. Error bars represent ± one standard deviation from the average of triplicate tests.

325

326 To better discern the environmentally-relevant release process, the impact of solution chemistry
 327 including pH, phosphate, carbonate, and tannic acid on the photo-dissolution kinetics was further
 328 examined. The photo-dissolution process was highly pH-dependent (Figure 6a). There was no

329 significant change of the photo-dissolution rate in acidic conditions as the initial pH increased from 4.92
330 ± 0.03 to 6.95 ± 0.02 . However, photo-dissolution drastically decreased as the initial pH increased from
331 6.95 ± 0.02 to 10.06 ± 0.02 . This could be attributed to the reduced valence band edge of the pigment,
332 which decreases from +1.02 V (NHE) to +0.84 V (NHE) as pH increases from 7 to 10. Nevertheless, the
333 photogenerated holes are still able to oxidize the cadmium pigment at pH 10 since the standard potential
334 for anodic dissolution of cadmium chalcogenide is around +0.32 V vs. NHE.^{43, 48} Another potential
335 offsetting mechanism is the formation of Cd(OH)₂ precipitates (K_{sp} , Cd(OH)₂ = 7.2×10^{-15})⁵² or sorption
336 of OH⁻ on the particle surfaces under alkaline conditions.⁵⁰ These processes effectively blocked the
337 surface sites suitable for trapping holes, leading to higher recombination of excitons and consequently
338 less reaction with surface trapped holes.²² Consistently, the XPS measurements suggest the atomic ratio
339 of oxygen in hydroxide to cadmium on the pigment surface increased from 34.2% to 55.0% after 1 h
340 irradiation at pH 10 (Figure S6). For experiments done at initial pH of 10.06 ± 0.02 , the photo-
341 dissolution process was slow during the initial 2 h, and then drastically increased afterwards. This is
342 because the overall reaction releases protons (Equation 8) and lowers the pH of the system, facilitating
343 the photo-dissolution process. The final pH of the samples with initial pH of 10.06 ± 0.02 was $6.81 \pm$
344 0.09 , consistent with this argument.

345 Naturally occurring anions including phosphate and carbonate significantly affected the photo-
346 dissolution process. The release of Cd²⁺ from cadmium sulfoselenide pigment during simulated sunlight
347 irradiation was inhibited in the presence of 10 mg/L phosphate or carbonate species (Figure 6b). The
348 inhibitory effect of phosphate and carbonate was exacerbated as their concentration was further
349 increased to 200 mg/L. The inhibition mechanism is the formation of photo-stable cadmium salts, which
350 are highly insoluble in water (K_{sp} , Cd₃(PO₄)₂ = 2.5×10^{-33} , and K_{sp} , CdCO₃ = 5.7×10^{-13}).^{53, 54} Meanwhile,
351 the anions in these cadmium salts, PO₄³⁻ and CO₃²⁻, cannot be oxidized by photogenerated holes. As a
352 result, these insoluble and photo-stable cadmium salts can passivate the pigment surface, inhibiting the
353 oxidation of cadmium sulfoselenide and the consequent release of Cd²⁺.

354 The presence of 20 mg/L tannic acid, a surrogate for dissolved organic matter (DOM),⁵⁵ inhibited the
355 photo-dissolution of cadmium sulfoselenide pigment. The inhibitory effect can be attributed to two
356 mechanisms. Tannic acid molecules can absorb light, exerting a screening effect. This decreases the
357 amount of photons received by pigment particles and consequently hinders the photo-dissolution
358 process. Furthermore, tannic acid is a plant polyphenol with antioxidant properties.⁵⁶ It can scavenge
359 photogenerated holes, mitigating oxidation of the pigment.⁵⁷ On the other hand, photoactive DOM can
360 produce phototransients such as singlet oxygen, hydrogen peroxide, hydroxyl radical, and superoxide,⁵⁸
361 which could enhance the oxidative dissolution of pigment particles. The overall effect of photoactive
362 DOM will depend on the interplay of its screening, hole scavenging, and photoactivity.

363 **Photo-dissolution of commercial cadmium sulfoselenide pigment in a natural setting**

364 In order to gain further insight into the natural photo-dissolution process of commercial cadmium
365 sulfoselenide pigment, we carried out a solar irradiation experiment with a river water sample on the
366 campus of Nanjing University from 11 a.m. to 3 p.m. on 11/04/2016. The solar irradiance was in the
367 range of 35.8 to 56.1 mW/cm² (Figure S7). The natural river water had pH of 7.70 ± 0.20 and total
368 organic carbon of 3.99 ± 0.32 mg/L. The concentrations of phosphate and carbonate ions in the river
369 water were 0.65 ± 0.04 mg/L and 271.87 ± 9.34 mg/L, respectively. Fast release kinetics of Cd²⁺ was
370 observed in this river water sample under natural solar irradiation, with 38.6 ± 0.1 % of the cadmium in
371 the pigment being released within 4 h (Figure S8). Thus, we provide unequivocal evidence of fast and
372 significant cadmium release from commercial cadmium sulfoselenide pigments under natural conditions.

373 **Environmental implications**

374 The commercial cadmium sulfoselenide pigment is photoactive under solar irradiation and is
375 susceptible to photo-dissolution, which is the key environmental process controlling its release of Cd²⁺.
376 The release can be mitigated by an increase in pH and the presence of anions that can form insoluble
377 and photo-stable salts with Cd²⁺. Once released into aquatic systems, commercial cadmium pigment will
378 undergo significant photo-dissolution within short period of time. The majority part of it will not persist

379 in the particulate form in natural settings, but will convert to highly toxic and bioavailable Cd²⁺. Thus,
380 current risk assessments and regulations of cadmium pigments and other semiconductor pigments with
381 hazardous metals need to consider their photochemistry. Our ongoing field investigation and a previous
382 study⁵⁹ show extensive use and potential discharge of cadmium pigments in several Chinese cities with
383 a booming ceramic industry.⁵⁹ We postulate that photo-dissolution is one of the environmental processes
384 that lead to the significant accumulation of cadmium in soils at several sites in these cities. Furthermore,
385 sunlight exposure of materials containing cadmium pigments could lead to potential environmental risks
386 and health concerns. Little is known about the extent to which the matrix such as polymers and ceramics
387 can inhibit the photo-dissolution of cadmium pigments and the subsequent release of metals. Future
388 research is needed to quantify the photo-induced release of toxic Cd²⁺ from colored products containing
389 cadmium pigments.

390

391 **ASSOCIATED CONTENT**

392 **Supporting Information**

393 The experimental setup for irradiation experiments, the spectrum of the Xeon lamp used in this study
394 and solar irradiation, the photo-dissolution kinetics of commercial cadmium sulfoselenide pigments
395 from different vendors, the ζ -potential of the commercial cadmium sulfoselenide pigment as a function
396 of irradiation time, the detection of O₂^{•-}, •OH, and H₂O₂ using probe molecules, the XPS spectrum of
397 the O1s peak of the pigment at different conditions, the variation of solar light power density during the
398 natural light exposure, the dissolution kinetics of commercial cadmium sulfoselenide pigment in natural
399 river water sample under solar irradiation, the cadmium release kinetics of the pigment under dark
400 condition at initial pH of 4.92, and the determination of pseudo-second-order reaction rate constant can
401 be found in the Supporting Information. This material is available free of charge via Internet at
402 <http://pubs.acs.org/>.

403

404 **AUTHOR INFORMATION**

405 **Corresponding Author**

406 *Xiaolei Qu; Phone: +86-025-8968-0256; email: xiaoleiqu@nju.edu.cn

407

408 **Acknowledgements**

409 This work was supported by the National Key Basic Research Program of China (Grant
410 2014CB441103), the National Natural Science Foundation of China (Grant 21622703, 21407073,
411 21225729, 21237002, and 21507056), the Department of Science and Technology of Jiangsu Province
412 (BE2015708), and the NSF ERC on Nanotechnology-Enabled Water Treatment (EEC-1449500). We
413 thank the State Key Laboratory of Environmental Chemistry and Ecotoxicology, Research Center for
414 Eco-Environmental Sciences, Chinese Academy of Sciences for partial funding (KF2014-11).

415

416 **Literature Cited**

- 417 (1) Jansen, M.; Letschert, H. P., Inorganic yellow-red pigments without toxic metals. *Nature* **2000**,
418 *404*, 980-982.
- 419 (2) Faulkner, E. B.; Schwartz, R. J., *High performance pigments*. John Wiley & Sons: 2009.
- 420 (3) EPA, Cadmium iris summary. *CASRN 7440-43-9* **1987**.
- 421 (4) Lu, Z. Z.; Xu, J.; Xie, X.; Wang, H. K.; Wang, C. D.; Kwok, S. Y.; Wong, T.; Kwong, H. L.;
422 Bello, I.; Lee, C. S.; Lee, S. T.; Zhang, W. J., Cds/cdse double-sensitized zno nanocable arrays
423 synthesized by chemical solution method and their photovoltaic applications. *J. Phys. Chem. C* **2012**,
424 *116*, 2656-2661.
- 425 (5) Ltd, W. A. I., Assessment of the risks to health and to the environment of cadmium contained in
426 certain products and of the effects of further restrictions on their marketing and use. **1998**.
- 427 (6) Wilson, D. C.; Young, P. J.; Hudson, B. C.; Baldwin, G., Leaching of cadmium from pigmented
428 plastics in a landfill site. *Environ. Sci. Technol.* **1982**, *16*, 560-566.
- 429 (7) Fleig, I.; Rieth, H.; Stocker, W. G.; Thiess, A. M., Chromosome investigations of workers
430 exposed to cadmium in the manufacturing of cadmium stabilizers and pigments. *Ecotox. Environ. Safe.*
431 **1983**, *7*, 106-110.
- 432 (8) Kawasaki, T.; Kono, K.; Dote, T.; Usuda, K.; Shimizu, H.; Dote, E., Markers of cadmium
433 exposure in workers in a cadmium pigment factory after changes in the exposure conditions. *Toxicol.*
434 *Ind. Health* **2004**, *20*, 51-56.
- 435 (9) Swafford, L. A.; Weigand, L. A.; Bowers, M. J.; McBride, J. R.; Rapaport, J. L.; Watt, T. L.;
436 Dixit, S. K.; Feldman, L. C.; Rosenthal, S. J., Homogeneously alloyed cdsxse1-(x) nanocrystals:
437 Synthesis, characterization, and composition/size-dependent band gap. *J. Am. Chem. Soc.* **2006**, *128*,
438 12299-12306.
- 439 (10) Eastaugh, N.; Walsh, V.; Chaplin, T.; Siddall, R., *Pigment compendium: A dictionary of*

- 440 *historical pigments*. Routledge: 2007.
- 441 (11) Mane, R. S.; Lokhande, C. D., Studies on chemically deposited cadmium sulphoselenide (cdsse)
442 films. *Thin Solid Films* **1997**, *304*, 56-60.
- 443 (12) Khot, K. V.; Mali, S. S.; Pawar, N. B.; Kharade, R. R.; Mane, R. M.; Patil, P. B.; Patil, P. S.;
444 Hong, C. K.; Kim, J. H.; Heo, J.; Bhosale, P. N., Simplistic construction of cadmium sulfoselenide thin
445 films via a hybrid chemical process for enhanced photoelectrochemical performance. *RSC Adv.* **2015**, *5*,
446 40283-40296.
- 447 (13) Hossain, M. A.; Jennings, J. R.; Mathews, N.; Wang, Q., Band engineered ternary solid solution
448 cdsxse_{1-x}-sensitized mesoscopic tio₂ solar cells. *Phys. Chem. Chem. Phys.* **2012**, *14*, 7154-7161.
- 449 (14) Li, Y.; Zhang, W.; Li, K.; Yao, Y.; Niu, J.; Chen, Y., Oxidative dissolution of polymer-coated
450 cdse/zns quantum dots under uv irradiation: Mechanisms and kinetics. *Environmental Pollution* **2012**,
451 *164*, 259-266.
- 452 (15) Matsumoto, H.; Sakata, T.; Mori, H.; Yoneyama, H., Preparation of monodisperse cds
453 nanocrystals by size selective photocorrosion. *The Journal of Physical Chemistry* **1996**, *100*, 13781-
454 13785.
- 455 (16) Spathis, P.; Poulios, I., The corrosion and photocorrosion of zinc and zinc oxide coatings.
456 *Corrosion Science* **1995**, *37*, 673-680.
- 457 (17) Peng, X.; Schlamp, M. C.; Kadavanich, A. V.; Alivisatos, A. P., Epitaxial growth of highly
458 luminescent cdse/cds core/shell nanocrystals with photostability and electronic accessibility. *J. Am.*
459 *Chem. Soc.* **1997**, *119*, 7019-7029.
- 460 (18) Xu, L.; Chen, K.; El-Khair, H. M.; Li, M.; Huang, X., Enhancement of band-edge luminescence
461 and photo-stability in colloidal cdse quantum dots by various surface passivation technologies. *Applied*
462 *Surface Science* **2001**, *172*, 84-88.
- 463 (19) Toma, F. M.; Cooper, J. K.; Kunzelmann, V.; McDowell, M. T.; Yu, J.; Larson, D. M.; Borys,
464 N. J.; Abelyan, C.; Beeman, J. W.; Yu, K. M.; Yang, J.; Chen, L.; Shaner, M. R.; Spurgeon, J.; Houle,
465 F. A.; Persson, K. A.; Sharp, I. D., Mechanistic insights into chemical and photochemical
466 transformations of bismuth vanadate photoanodes. *Nature Communications* **2016**, *7*, 12012.
- 467 (20) Fermín, D. J.; Ponomarev, E. A.; Peter, L. M., A kinetic study of cds photocorrosion by intensity
468 modulated photocurrent and photoelectrochemical impedance spectroscopy. *Journal of*
469 *Electroanalytical Chemistry* **1999**, *473*, 192-203.
- 470 (21) Meissner, D.; Memming, R.; Kastening, B., Photoelectrochemistry of cadmium sulfide. 1.
471 Reanalysis of photocorrosion and flat-band potential. *The Journal of Physical Chemistry* **1988**, *92*,
472 3476-3483.
- 473 (22) Spanhel, L.; Haase, M.; Weller, H.; Henglein, A., Photochemistry of colloidal semiconductors
474 .20. Surface modification and stability of strong luminescing cds particles. *J. Am. Chem. Soc.* **1987**, *109*,
475 5649-5655.
- 476 (23) Manner, V. W.; Kopusov, A. Y.; Szymanski, P.; Klimov, V. I.; Sykora, M., Role of solvent-
477 oxygen ion pairs in photooxidation of cdse nanocrystal quantum dots. *ACS Nano* **2012**, *6*, 2371-2377.
- 478 (24) Xi, L. F.; Lek, J. Y.; Liang, Y. N.; Boothroyd, C.; Zhou, W. W.; Yan, Q. Y.; Hu, X.; Chiang, F.
479 B. Y.; Lam, Y. M., Stability studies of cdse nanocrystals in an aqueous environment. *Nanotechnology*
480 **2011**, *22*, 5.
- 481 (25) Derfus, A. M.; Chan, W. C. W.; Bhatia, S. N., Probing the cytotoxicity of semiconductor
482 quantum dots. *Nano Letters* **2004**, *4*, 11-18.
- 483 (26) Shang, E.; Niu, J.; Li, Y.; Zhou, Y.; Crittenden, J. C., Comparative toxicity of cd, mo, and w
484 sulphide nanomaterials toward e. coli under uv irradiation. *Environmental Pollution* **2017**, *224*, 606-
485 614.
- 486 (27) Meissner, D.; Memming, R.; Shuben, L.; Yesodharan, S.; Grätzel, M., Photocorrosion by
487 oxygen uptake in aqueous cadmium sulphide suspensions. *Berichte der Bunsengesellschaft für*
488 *physikalische Chemie* **1985**, *89*, 121-124.
- 489 (28) Anaf, W.; Trashin, S.; Schalm, O.; van Dorp, D.; Janssens, K.; De Wael, K., Electrochemical
490 photodegradation study of semiconductor pigments: Influence of environmental parameters. *Analytical*

- 491 *Chemistry* **2014**, *86*, 9742-9748.
- 492 (29) Van der Snickt, G.; Dik, J.; Cotte, M.; Janssens, K.; Jaroszewicz, J.; De Nolf, W.; Groenewegen,
493 J.; Van der Loeff, L., Characterization of a degraded cadmium yellow (c_{ds}) pigment in an oil painting
494 by means of synchrotron radiation based x-ray techniques. *Analytical Chemistry* **2009**, *81*, 2600-2610.
- 495 (30) Van der Snickt, G.; Janssens, K.; Dik, J.; De Nolf, W.; Vanmeert, F.; Jaroszewicz, J.; Cotte, M.;
496 Falkenberg, G.; Van der Loeff, L., Combined use of synchrotron radiation based micro-x-ray
497 fluorescence, micro-x-ray diffraction, micro-x-ray absorption near-edge, and micro-fourier transform
498 infrared spectroscopies for revealing an alternative degradation pathway of the pigment cadmium
499 yellow in a painting by van gogh. *Analytical Chemistry* **2012**, *84*, 10221-10228.
- 500 (31) Sutherland, M. W.; Learmonth, B. A., The tetrazolium dyes mts and xtt provide new quantitative
501 assays for superoxide and superoxide dismutase. *Free Radic. Res.* **1997**, *27*, 283-289.
- 502 (32) Haag, W. R.; Hoigné, J., Photo-sensitized oxidation in natural water via .Oh radicals.
503 *Chemosphere* **1985**, *14*, 1659-1671.
- 504 (33) Zepp, R. G.; Schlotzhauer, P. F.; Sink, R. M., Photosensitized transformations involving
505 electronic-energy transfer in natural-waters - role of humic substances. *Environ. Sci. Technol.* **1985**, *19*,
506 74-81.
- 507 (34) Chen, C.-Y.; Jafvert, C. T., Photoreactivity of carboxylated single-walled carbon nanotubes in
508 sunlight: Reactive oxygen species production in water. *Environ. Sci. Technol.* **2010**, *44*, 6674-6679.
- 509 (35) Hsieh, H. S.; Wu, R. R.; Jafvert, C. T., Light-independent reactive oxygen species (ros)
510 formation through electron transfer from carboxylated single-walled carbon nanotubes in water.
511 *Environ. Sci. Technol.* **2014**, *48*, 11330-11336.
- 512 (36) Derjaguin, B.; Landau, L., Theory of stability of highly charged liophobic sols and adhesion of
513 highly charged particles in solutions of electrolytes. *Zhurnal Eksperimentalnoi Teor. Fiz.* **1945**, *15*, 663-
514 682.
- 515 (37) Verwey, E. J. W., Theory of the stability of lyophobic colloids. *Philips Research Reports* **1945**,
516 *1*, 33-49.
- 517 (38) Kevin, P.; Alghamdi, Y. G.; Lewis, D. J.; Azad Malik, M., Morphology and band gap controlled
518 aacvd of cdse and cdsxel-x thin films using novel single source precursors:
519 Bis(diethyldithio/diselenocarbamate)cadmium(ii). *Materials Science in Semiconductor Processing*
520 **2015**, *40*, 848-854.
- 521 (39) Zou, Z.; Ye, J.; Sayama, K.; Arakawa, H., Direct splitting of water under visible light irradiation
522 with an oxide semiconductor photocatalyst. *Nature* **2001**, *414*, 625-627.
- 523 (40) Kubelka, P., New contributions to the optics of intensely light-scattering materials. Part i. *J. Opt.*
524 *Soc. Am.* **1948**, *38*, 448-457.
- 525 (41) López, R.; Gómez, R., Band-gap energy estimation from diffuse reflectance measurements on
526 sol-gel and commercial tio₂: A comparative study. *Journal of Sol-Gel Science and Technology* **2012**,
527 *61*, 1-7.
- 528 (42) Bott, A. W., Electrochemistry of semiconductors. *Current Separations* **1998**, *17*, 87-92.
- 529 (43) Xu, Y.; Schoonen, M. A. A., The absolute energy positions of conduction and valence bands of
530 selected semiconducting minerals. *Am. Miner.* **2000**, *85*, 543-556.
- 531 (44) Kamat, P. V., Photochemistry on nonreactive and reactive (semiconductor) surfaces. *Chemical*
532 *Reviews* **1993**, *93*, 267-300.
- 533 (45) Makino, K.; Hagiwara, T.; Murakami, A., A mini review: Fundamental aspects of spin trapping
534 with dmpo. *International Journal of Radiation Applications and Instrumentation. Part C. Radiation*
535 *Physics and Chemistry* **1991**, *37*, 657-665.
- 536 (46) Zhao, J. F.; Zhang, B. W.; Li, J. Y.; Liu, Y. C.; Wang, W. F., Photo-enhanced oxidizability of
537 tetrazolium salts and its impact on superoxide assaying. *Chem. Commun.* **2016**, *52*, 11595-11598.
- 538 (47) Kim, J.; Lee, C. W.; Choi, W., Platinized wo₃ as an environmental photocatalyst that generates
539 oh radicals under visible light. *Environ. Sci. Technol.* **2010**, *44*, 6849-6854.
- 540 (48) Bard, A. J.; Wrighton, M. S., Thermodynamic potential for the anodic dissolution of n-type
541 semiconductors. *Journal of the Electrochemical Society* **1977**, *124*, 1706-1710.

- 542 (49) Tan, Y.; Jin, S.; Hamers, R. J., Influence of hole-sequestering ligands on the photostability of
543 cdse quantum dots. *The Journal of Physical Chemistry C* **2013**, *117*, 313-320.
- 544 (50) Torimoto, T.; Nishiyama, H.; Sakata, T.; Mori, H.; Yoneyama, H., Characteristic features of
545 size-selective photoetching of cds nanoparticles as a means of preparation of monodisperse particles.
546 *Journal of the Electrochemical Society* **1998**, *145*, 1964-1968.
- 547 (51) Belabed, C.; Rekhila, G.; Doulache, M.; Zitouni, B.; Trari, M., Photo-electrochemical
548 characterization of polypyrrol: Application to visible light induced hydrogen production. *Solar Energy*
549 *Materials and Solar Cells* **2013**, *114*, 199-204.
- 550 (52) Lide, D. R., *Crc handbook of chemistry and physics*. CRC press: 2004; Vol. 85.
- 551 (53) Eighmy, T. T.; Eusden, J. D.; Krzanowski, J. E.; Domingo, D. S.; Staempfli, D.; Martin, J. R.;
552 Erickson, P. M., Comprehensive approach toward understanding element speciation and leaching
553 behavior in municipal solid waste incineration electrostatic precipitator ash. *Environ. Sci. Technol.*
554 **1995**, *29*, 629-646.
- 555 (54) Street, J. J.; Lindsay, W. L.; Sabey, B. R., Solubility and plant uptake of cadmium in soils
556 amended with cadmium and sewage sludge. *J. Environ. Qual.* **1977**, *6*, 72-77.
- 557 (55) Yamamoto, H.; Liljestrand, H. M.; Shimizu, Y.; Morita, M., Effects of physical-chemical
558 characteristics on the sorption of selected endocrine disruptors by dissolved organic matter surrogates.
559 *Environ. Sci. Technol.* **2003**, *37*, 2646-2657.
- 560 (56) Hagerman, A. E.; Riedl, K. M.; Jones, G. A.; Sovik, K. N.; Ritchard, N. T.; Hartzfeld, P. W.;
561 Riechel, T. L., High molecular weight plant polyphenolics (tannins) as biological antioxidants. *Journal*
562 *of Agricultural and Food Chemistry* **1998**, *46*, 1887-1892.
- 563 (57) Long, M.; Brame, J.; Qin, F.; Bao, J.; Li, Q.; Alvarez, P. J. J., Phosphate changes effect of humic
564 acids on tio2 photocatalysis: From inhibition to mitigation of electron-hole recombination. *Environ. Sci.*
565 *Technol.* **2017**, *51*, 514-521.
- 566 (58) Zhou, H.; Lian, L.; Yan, S.; Song, W., Insights into the photo-induced formation of reactive
567 intermediates from effluent organic matter: The role of chemical constituents. *Water Research* **2017**,
568 *112*, 120-128.
- 569 (59) Liao, Q. L.; Liu, C.; Wu, H. Y.; Jin, Y.; Hua, M.; Zhu, B. W.; Chen, K.; Huang, L., Association
570 of soil cadmium contamination with ceramic industry: A case study in a chinese town. *Sci. Total*
571 *Environ.* **2015**, *514*, 26-32.

572

